JOURNAL OF AIRCRAFT
Vol. 41, No. 4, July–August 2004

Flutter Analysis of Aircraft with External Stores Using Modal Coupling

M. Karpel* and B. Moulin†
Technion—Israel Institute of Technology, Haifa 32000, Israel
and
L. Anguita,‡ C. Maderuelo,‡ and H. Climent§
EADS–CASA, 28906 Madrid, Spain

A new modal coupling technique for efficient flutter and aeroservoelastic analyses of aircraft with multiple external-store configurations is presented. The aircraft is represented by a set of free–free normal modes obtained with large fictitious masses loading the interface coordinates to yield high-accuracy subsequent coupling results. Each store is represented by its own vibration modes obtained with a subset of statically determined interface coordinates clamped to the ground, and the remaining coordinates (if any) are loaded with large fictitious masses. The technique is formulated in a way that facilitates its application using standard options of common commercially available software packages. A finite element code is used to construct the aircraft and stores modal databases. A linear unsteady aerodynamics code is used to read the modal information, calculate the aerodynamic databases, construct and solve the aircraft–store coupling equations, and perform frequency-domain and state-space flutter analyses with or without control system effects. The process allows analyzing numerous store configurations with previously stored structural and aerodynamic databases, with the store aerodynamics taken into account. The method accuracy and efficiency are demonstrated with a model of the Euro Fighter EF-2000 with four wing store stations.

Introduction

FIGHTER aircraft are required to carry numerous combinations of wing-mounted external stores. The task of flutter clearance requires repeated stability analyses for thousands of store combinations at several points in the flight envelope and, possibly, with various control–system effects. Common flutter analysis methods are based on the modal approach in which the structural degrees of freedom are represented by a set of low-frequency normal modes of the analyzed configuration.[1] Because different store configurations have different natural frequencies and mode shapes, the standard procedures require the flutter evaluation of each store configuration to start with normal modes analysis at the finite element model level. The enormous amounts of associated computation time, pre- and postdata processing efforts, and result evaluation work make the full consideration of all external-store-related structural, aerodynamic, and control effects during the aircraft design stages practically impossible. A complete flutter evaluation performed only at the end of the design process might require costly aerodynamic, structural, and/or control system changes, or flight envelope limitations.

A way to shorten the repeated analysis process is by modal coupling of a set of low-frequency aircraft modes with those of the separate external stores. The main difficulty in modal coupling is that the modal information has to include local deformations around the component interface points to yield adequate coupling results. Common modal coupling methods such as that of Craig and Bampton[2] supplemented the component modes by static interface constraint modes in which unit displacements are applied to the interface coordinates one at a time. The involvement of static modes and some special features needed for treating free–free structures made it difficult to apply with standard aeroelastic codes. The fictitious-mass modal-coupling method[3] made possible the local deformations around selected grid points in the low-frequency normal modes to be taken into account. The application of this approach to vibration mode analysis of aircraft with external stores[4] exhibited very accurate results for a variety of store loading, all based on the same set of modes of the clean aircraft that is loaded with fictitious masses at the hard points. The fictitious-mass coupling method was also applied with measured modes from vibration tests of components loaded with boundary masses.[5,6] The fictitious-mass concept was generalized in Ref. 7 by the definition of a special finite element that can be used in structural dynamic models where deformations at a small number of discrete degrees of freedom are of special interest.

Various aircraft manufacturers developed in-house procedures to increase the efficiency of repeated store flutter analysis. The problems with these procedures are that 1) analysis details and the associated software codes are not available to others, 2) they are not compatible with the software of other manufacturers, and 3) they might not be readily applicable in modern procedures for aeroservoelastic analysis. Hence, the usefulness of these procedures in a cooperative design process of modern control-augmented aircraft that involves several manufacturers is limited.

The ZAERO aeroelastic analysis software package[8] provides a platform for the development of a new aircraft–store flutter procedure that can be applied in any aeronautics industry environment. The package can read modal data generated by any finite element code. The unsteady aerodynamics associated with these modes are either generated within the package or read in from user-supplied files. The store aerodynamics can be calculated for each store separately and then combined in the coupling process. There is an option of running several flutter cases in which different mass terms are added to a baseline structure with a fixed set of normal modes. State-space aeroservoelastic analyses are efficiently performed within the code.

Presented as Paper 2002-1597 at the AIAA/ASME/ASCE/AHS/ASC 43rd Structures, Structural Dynamics and Material Conference, Denver, CO, 22–25 April 2002; received 24 July 2002; revision received 25 September 2003; accepted for publication 6 October 2003.

*Professor, Sanford Kaplan Chair in Aerospace Engineering. Associate Fellow AIAA.
†Senior Researcher, Faculty of Aerospace Engineering. Member AIAA.
‡Senior Aeroservoelastic Specialist, Aeroelasticity and Structural Dynamics Department, John Lennon s/n, Getafe.
§Head, Aeroelasticity and Structural Dynamics Department, John Lennon s/n, Getafe.

The purposes of the work presented in this paper were 1) to reformulate the aircraft–store modal coupling method of Ref. 4 to be based on standard added-mass features, 2) to expand the method to allow overdetermined wing–store connections, 3) to define an efficient procedure for including store aerodynamic effects in the modal coupling process, 4) to allow efficient repeated flutter analyses using both frequency-domain and aeroservoelastic (ASE) state-space methods, and 5) demonstrate the new method by applying it to industrial cases.

Modal Coupling with Statically Determined Interface

The aircraft–store modal coupling technique of Ref. 4 is modified in this section to be based on standard added-mass features. The technique couples the normal modes of the aircraft, obtained with the aircraft–store interface coordinates loaded with large fictitious masses, with those of the separate external stores, clamped to the ground at the interface coordinates. The fictitious masses and coupling equations are reviewed in this section, where it is assumed that the aircraft–store interfaces are statically determinate, namely, the number of interface coordinates is equal to the number of free–free store rigid-body modes. Overdetermined connections are discussed in the next section. For the sake of simplicity, we assume at this stage that a single external store is to be connected to a store station on the wing of an aircraft model with either symmetric or anti-symmetric boundary conditions applied at the plane of symmetry.

The normal modes of the clean aircraft satisfy the eigenvalue equation

$$\begin{bmatrix} K_{AA} & K_{AI} \\ K_{AI}^T & K_{II}^{(A)} \end{bmatrix} \begin{bmatrix} \phi_A \\ \phi_I \end{bmatrix} = \begin{bmatrix} M_{AA} & M_{AI} \\ M_{AI}^T & M_{II}^{(A)} + M_F \end{bmatrix} \begin{bmatrix} \phi_A \\ \phi_I \end{bmatrix} [\Omega_A] \tag{1}$$

where $[K]$ and $[M]$ are the finite element stiffness and mass matrices and $[\phi]$ is the matrix of aircraft modes taken into account. The subscripts A and I relate to the aircraft and the interface coordinates, respectively, $[M_F]$ is a matrix of fictitious masses loading the interface coordinates, and Ω_A is a diagonal matrix of the eigenvalues associated with the normal modes. The fictitious masses should be similar to, or larger than, the heaviest stores to be mounted on the respective store station. In Ref. 4, it is shown that with large fictitious masses the subsequent coupling results are not sensitive to their values. However, extremely large fictitious masses (several orders of magnitude larger than the total aircraft masses) might cause numerical ill conditioning. The diagonal eigenvalue and generalized mass matrices satisfy

$$\left[M_{ii_A}\right] = \begin{bmatrix} \phi_A \\ \phi_{AI} \end{bmatrix}^T \begin{bmatrix} M_{AA} & M_{AI} \\ M_{AI}^T & M_{II}^{(A)} + M_F \end{bmatrix} \begin{bmatrix} \phi_A \\ \phi_{AI} \end{bmatrix} \tag{2}$$

$$[\Omega_A]\left[M_{ii_A}\right] = \begin{bmatrix} \phi_A \\ \phi_{AI} \end{bmatrix}^T \begin{bmatrix} K_{AA} & K_{AI} \\ K_{AI}^T & K_{II}^{(A)} \end{bmatrix} \begin{bmatrix} \phi_A \\ \phi_{AI} \end{bmatrix} \tag{3}$$

The normal modes of a separate store, B, clamped at its interface coordinates, satisfy the eigenvalue equation

$$\begin{bmatrix} K_{BB} & K_{BI} \\ K_{BI}^T & K_{II}^{(B)} \end{bmatrix} \begin{bmatrix} \phi_B \\ 0 \end{bmatrix} = \begin{bmatrix} M_{BB} & M_{BI} \\ M_{BI}^T & M_{II}^{(B)} \end{bmatrix} \begin{bmatrix} \phi_B \\ 0 \end{bmatrix} [\Omega_B] \tag{4}$$

where the diagonal eigenvalue and generalized mass matrices satisfy

$$\left[M_{ii_B}\right] = [\phi_B]^T [M_{BB}][\phi_B] \tag{5}$$

$$[\Omega_B]\left[M_{ii_B}\right] = [\phi_B]^T [K_{BB}][\phi_B] \tag{6}$$

The undamped free-vibration equation of motion of the combined structure, $A + B$ is

$$\begin{bmatrix} M_{AA} & M_{AI} & 0 \\ M_{AI}^T & M_{II}^{(A)} + M_{II}^{(B)} & M_{BI}^T \\ 0 & M_{BI} & M_{BB} \end{bmatrix} \begin{Bmatrix} \ddot{u}_A \\ \ddot{u}_I \\ \ddot{u}_B \end{Bmatrix} + \begin{bmatrix} K_{AA} & K_{AI} & 0 \\ K_{AI}^T & K_{II}^{(A)} + K_{II}^{(B)} & K_{BI}^T \\ 0 & K_{BI} & K_{BB} \end{bmatrix} \begin{Bmatrix} u_A \\ u_I \\ u_B \end{Bmatrix} = \{0\} \tag{7}$$

The modal-coupling technique assumes that the displacements of the combined structure are linear combinations of the separately obtained component modes

$$\begin{Bmatrix} u_A \\ u_I \\ u_B \end{Bmatrix} = \begin{bmatrix} \phi_A & 0 \\ \phi_{AI} & 0 \\ \phi_{AB} & \phi_B \end{bmatrix} \begin{Bmatrix} \xi_A \\ \xi_B \end{Bmatrix} \tag{8}$$

where $[\phi_{AB}]$ is the matrix of modal displacements at the store points, rigidly extrapolated from the interface modal displacements $[\phi_{AI}]$.

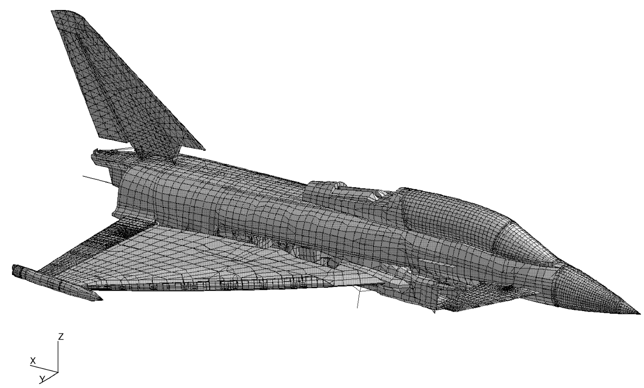

Fig. 1 EF-2000 finite element model.

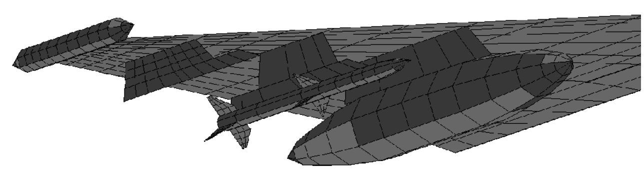

Fig. 2 Aerodynamic model of wing with three stores.

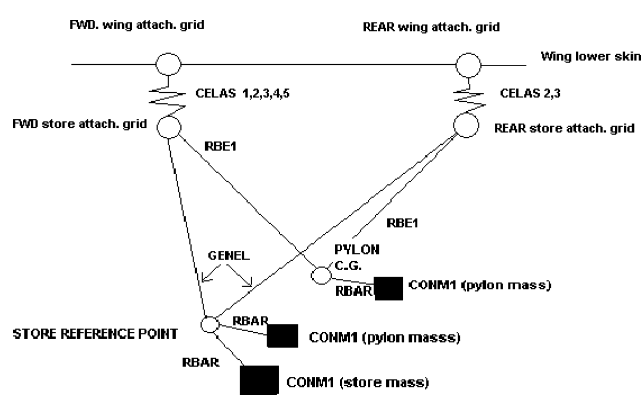

Fig. 3 Typical store model.

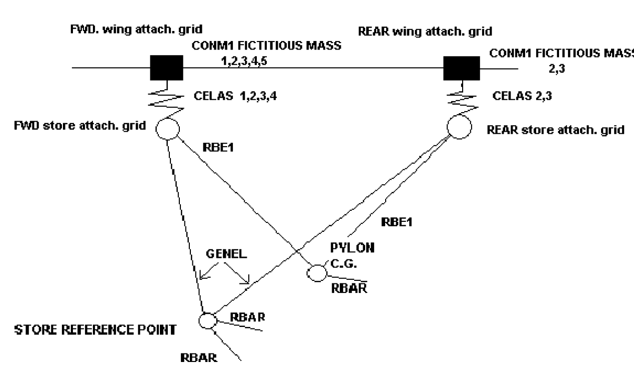

Fig. 4 Store ghost model with fictitious masses.

The substitution of Eq. (8) in Eq. (7), its premultiplication by the modes matrix, and the consideration of Eqs. (2–6) yield

$$\begin{bmatrix} M_{ii_A} - M_{ii_F} + M_{ii_{IB}} & M_{ii_{AB}} \\ M_{ii_{AB}}^T & M_{ii_B} \end{bmatrix} \begin{Bmatrix} \ddot{\xi}_A \\ \ddot{\xi}_B \end{Bmatrix} + \begin{bmatrix} \Omega_A M_{ii_A} & 0 \\ 0 & \Omega_B M_{ii_B} \end{bmatrix} \begin{Bmatrix} \xi_A \\ \xi_B \end{Bmatrix} = \{0\} \tag{9}$$

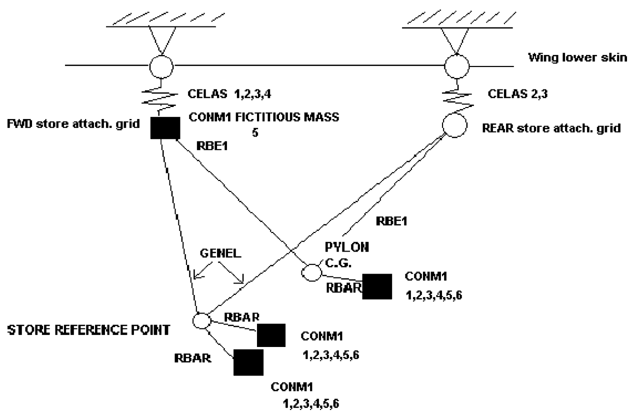

Fig. 5 Store model for separate store modes.

where

$$\left[M_{ii_F}\right] = [\phi_{AI}]^T [M_F][\phi_{AI}] \tag{10}$$

$$\begin{bmatrix} M_{ii_{IB}} & M_{ii_{AB}} \\ M_{ii_{AB}}^T & M_{ii_B} \end{bmatrix} = \begin{bmatrix} \phi_{AI} & 0 \\ \phi_{AB} & \phi_B \end{bmatrix}^T \begin{bmatrix} M_{II}^{(B)} & M_{BI}^T \\ M_{BI} & M_{BB} \end{bmatrix} \begin{bmatrix} \phi_{AI} & 0 \\ \phi_{AB} & \phi_B \end{bmatrix} \tag{11}$$

Equation (9) forms a reduced-size eigenvalue problem that can be solved for the eigenvalues and eigenvectors of the coupled system. The linear combination of Eq. (8) can be used to recover the discrete modal displacements from the coupled eigenvectors. Equation (9) can form the basis for a direct aeroelastic analyses of the coupled system. It can be observed that the expression for $[M_{ii_B}]$ is identical to that of Eq. (5). However, it is possible to use Eq. (11) with different masses than those used in Eq. (5) while the store modes are created. This facilitates the analysis of many mass variations of a certain store, that is, a fuel tank, with the same set of store modes.

Equation (11) can be easily expanded for cases of multiple stores. Each store station is loaded in the aircraft normal-modes analysis with its own set of fictitious masses. The store generalized displacement vector $\{\xi_B\}$ and the associated generalized matrices in Eq. (8) become the assembly of the modal matrices of the different stores. The case of no store at one or more of the stations can be analyzed by simply assigning no store modes at the respective stations and neglecting the effects of Eq. (11). The main advantage of the modal

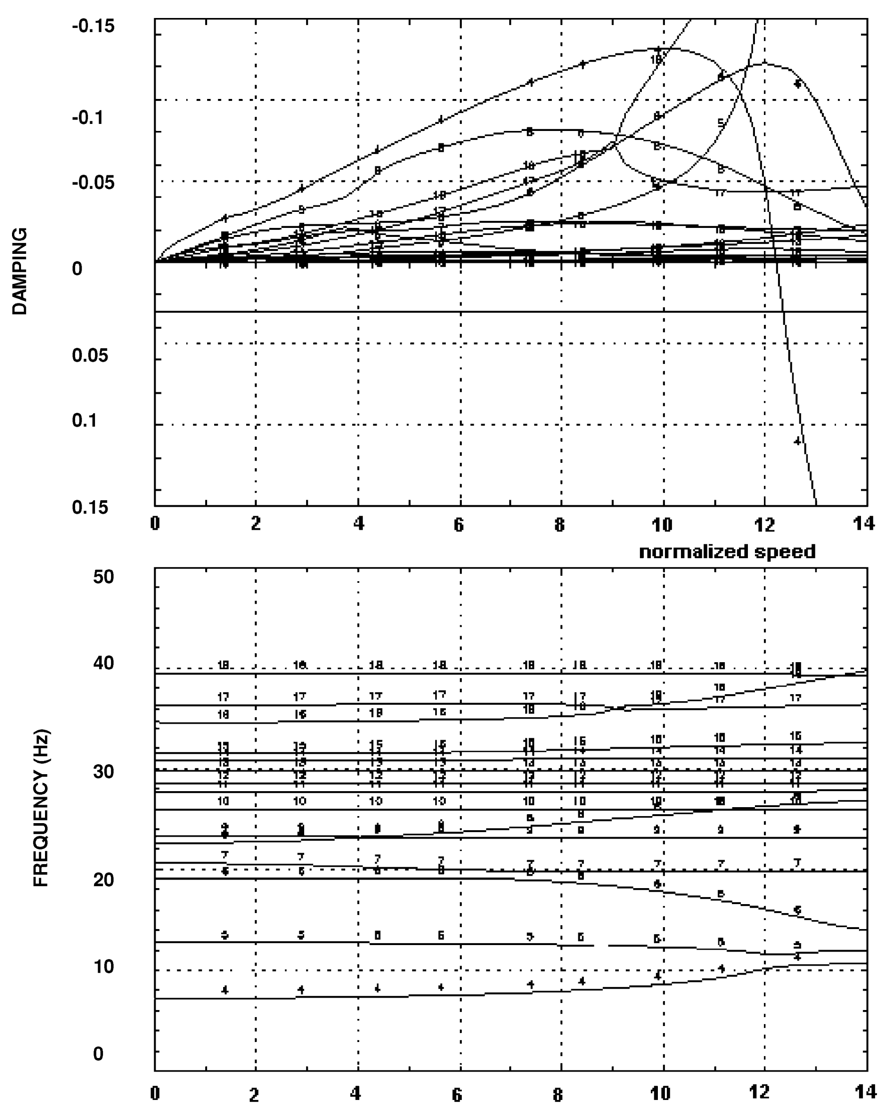

Fig. 6 Frequency and damping vs normalized velocity, clean aircraft direct solution.

coupling technique is that it allows normal-modes and aeroelastic analyses of many store combinations with the same set of aircraft modes, plus one set of modes for each external store.

Overdetermined Interface

Overdetermined connections might introduce undesired local stresses due to inaccurate pylon mounting in field conditions and due to elastic deformations in dynamic structural response to high maneuvers and store ejection. Hence, wing–pylon interfaces are often designed such that they can be considered as statically determined. Cases of overdetermined interface can still be handled by the procedure of the preceding section when the overdetermination has minor effects. The effects can be considered minor if the modal-coupling assumption of Eq. (8) is still adequate. The issues to be considered are 1) the use of the overdetermined interface modal displacements $[\phi_{AI}]$ for calculating $[\phi_{AB}]$, 2) the significance of the overdetermined stiffness effects, and 3) the sufficiency of elastic information contained in the clamped modes $[\phi_B]$ in representing the store dynamics.

A more accurate way to treat overdetermined connections is by adding stiff interconnection elements to the coupling equation (7). The interface coordinates are divided into a statically determined set and an additional-connection set. The additional-connection coordinates are modeled by two sets of collocated grid points that would be, in a regular aircraft–stores analysis, interconnected by spring elements. Whereas the wing side of the additional connections is still a part of the interface coordinates $\{u_I\}$ of Eq. (7), the store side is now a part of the internal store coordinates $\{u_B\}$. The spring elements that interconnect the additional interface coordinates are not included in the normal modes analyses that generate the aircraft and store modes of Eq. (8). Instead, they define incremental stiffness matrices $[\Delta K_{II}^{(B)}]$, $[\Delta K_{BI}]$, and $[\Delta K_{BB}]$ to be added in the subsequent coupling equation (12).

The fictitious masses added in Eq. (1) to the interface coordinates while calculating the aircraft modes should be applied to all of the wing-side interface coordinates. To improve the accuracy of the interface stiffness additions, the store-side added coordinates could be mounted with fictitious masses $[M_{FB}]$ when the clamped store modes $[\phi_B]$ are calculated. The effects of these fictitious masses are removed from the coupling equation (9) that, together with the added stiffness elements, becomes

$$\begin{bmatrix} M_{ii_A} - M_{ii_{FA}} + M_{ii_{IB}} & M_{ii_{AB}} \\ M_{ii_{AB}}^T & M_{ii_B} - M_{ii_{FB}} \end{bmatrix} \begin{Bmatrix} \ddot{\xi}_A \\ \ddot{\xi}_B \end{Bmatrix} + \begin{bmatrix} \Omega_A M_{ii_A} + \Delta K_{ii_{ib}} & \Delta K_{ii_{AB}} \\ \Delta K_{ii_{AB}}^T & \Omega_B M_{ii_B} + \Delta K_{ii_B} \end{bmatrix} \begin{Bmatrix} \xi_A \\ \xi_B \end{Bmatrix} = \{0\} \quad (12)$$

where

$$\left[M_{ii_{FB}}\right] = [\phi_B]^T [M_{FB}][\phi_B] \quad (13)$$

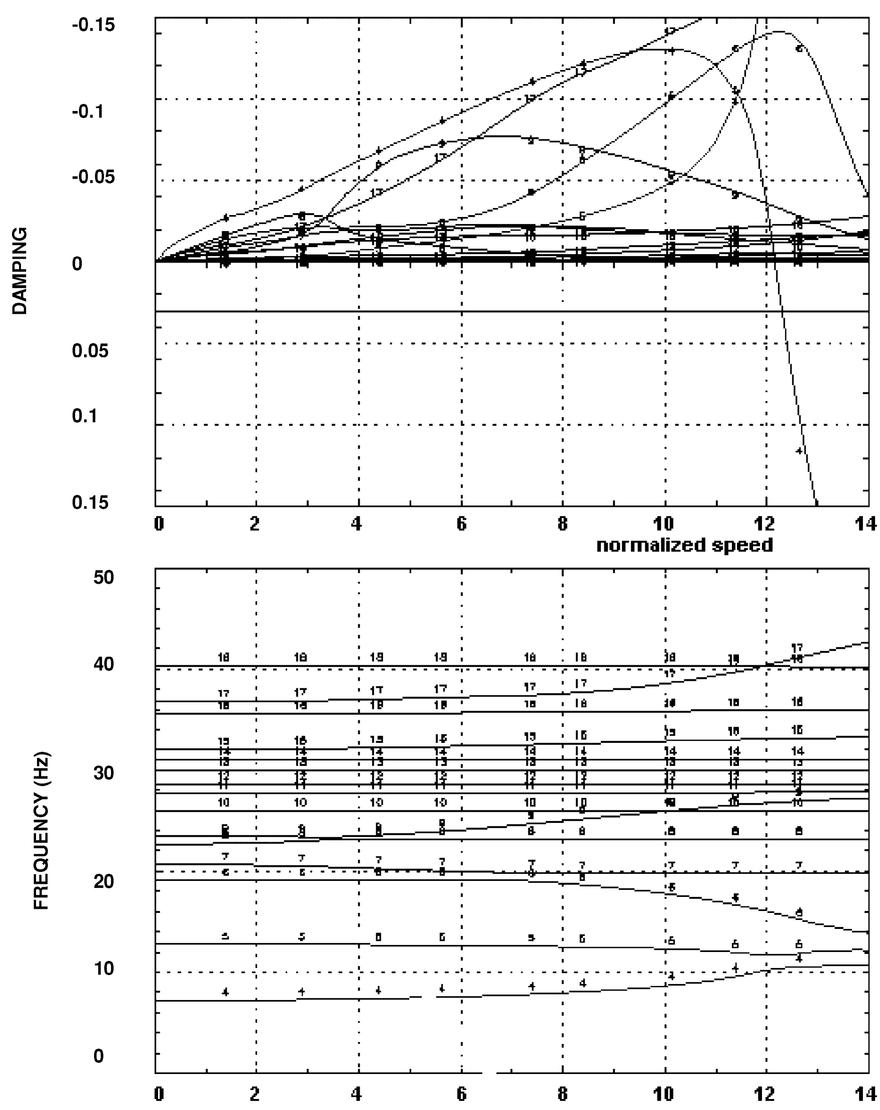

Fig. 7 Frequency and damping vs normalized velocity, clean aircraft by coupling.

$$
\begin{bmatrix} \Delta K_{ii_{IB}} & \Delta K_{ii_{AB}} \\ \Delta K_{ii_{AB}}^T & \Delta K_{ii_B} \end{bmatrix} = \begin{bmatrix} \phi_{IA} & 0 \\ \phi_{AB} & \phi_B \end{bmatrix}^T \times \begin{bmatrix} \Delta K_{II}^{(B)} & \Delta K_{BI}^T \\ \Delta K_{BI} & \Delta K_{BB} \end{bmatrix} \begin{bmatrix} \phi_{IA} & 0 \\ \phi_{AB} & \phi_B \end{bmatrix} \tag{14}
$$

Unsteady Aerodynamic Forces

Store flutter analysis requires the generalized aerodynamic force (GAF) coefficient matrices associated with the modal coordinates and the aerodynamic shapes of the specific store configurations. A cold-start computation process of GAF matrices for a store configuration includes panel modeling of the specific aerodynamic shape, generation of the respective aerodynamic force coefficient (AFC) matrices at several reduced frequencies, and using the AFC matrices and the specific structural modes for obtaining the GAF matrices. The application of this process to each store configuration would require unacceptable preparation and computation time.

The importance of considering the aerodynamics associated with external stores is assessed by combining previous experience, comparative flutter analyses with and without store aerodynamics, and wind-tunnel tests for selected configuration with actual and pencil shapes. The following approaches can be taken for treating the store aerodynamics in repetitive numerical store flutter analyses:

1) Neglect store aerodynamic effects, based on the assumptions that these effects are either small, namely, covered by the safety margins, or conservative.

2) Construct a database of AFC matrices associated with selected store configurations, and assume that each AFC set can represent a variety of store loadings. Each store case is assigned with a database aerodynamic shape.

3) Calculate the GAF matrices associated with the aircraft and store modes in Eq. (8) for each store separately, subtract the clean-aircraft GAF matrices, and combine the incremental effects in the flutter equations with the aerodynamic interference between different stores neglected.

The application of the three numerical approaches and their effects on accuracy and computation efficiency are demonstrated and discussed in the numerical example section.

Flutter Analysis

The Laplace domain open-loop generalized matrix equation of motion of an aeroelastic system, excited by control-surface displacements $\{\delta_c\}$, is

$$
\left(s^2[M_{hh}] + s[B_{hh}] + [K_{hh}] + q[Q_{hh}(s)]\right)\{\xi(s)\} = -\left(s^2[M_{hc}] + q[Q_{hc}(s)]\right)\{\delta_c(s)\} \tag{15}
$$

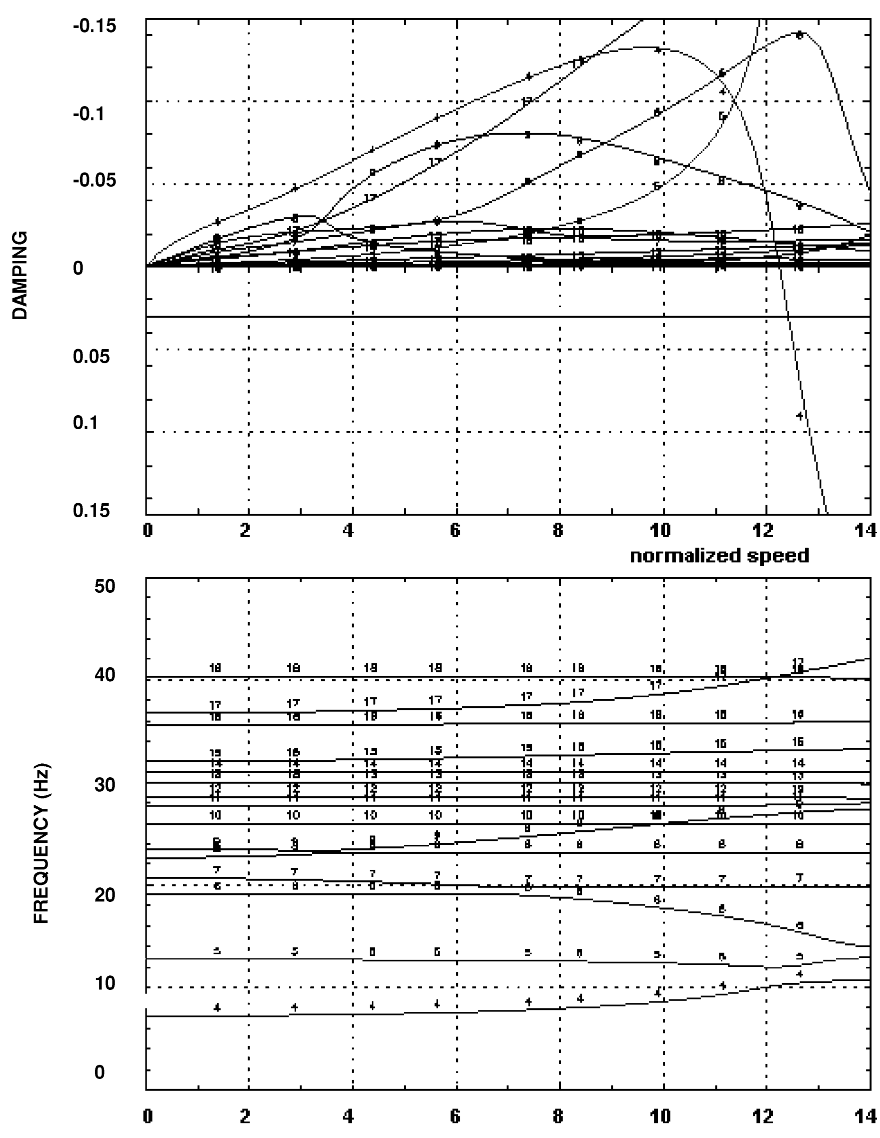

Fig. 8 Frequency and damping variations, clean aircraft by coupling, ASE solution.

where s is the Laplace variable; q is the dynamic pressure; V is the true air velocity; $\{\xi\}$ is the vector of generalized displacements of the n_h structural modes taken into account; $[M_{hh}]$, $[K_{hh}]$, $[B_{hh}]$, and $[Q_{hh}]$ are the associated generalized mass, damping, stiffness, and aerodynamic matrices; $\{\delta_c\}$ is the vector of control-surface rotation commands; and $[M_{hc}]$ and $[Q_{hc}]$ are the control mass and aerodynamic excitation matrices. When $\{\xi\}$ relates to natural modes of the analyzed structure, $[M_{hh}]$ and $[K_{hh}]$ are diagonal. To apply the aircraft–stores modal coupling technique, $\{\xi\}$ becomes the assembly of generalized displacements in Eq. (12), with the associated generalized mass and stiffness matrices forming $[M_{hh}]$ and $[K_{hh}]$, which become nondiagonal.

Common frequency-domain flutter analysis procedures determine the flutter boundaries by numerically searching for the velocity and frequency pairs where one of the eigenvalues of the left-hand coefficient matrix in Eq. (15) is purely imaginary. The search involves the interpolation of the tabulated GAF matrices according to the varying reduced frequency k and their extrapolation to the entire Laplace domain. The ZAERO code uses the g method[8] for solving the flutter equations. The AFC matrices can be obtained in ZAERO by combining the aircraft and store modes in the input data as in Eq. (8), with the original stiffness and mass matrices except that the store generalized masses are set to zero. The modal coupling is then expressed for each store configuration by defining the fictitious masses, with a negative sign, and the actual store masses as added masses at their respective grid points. When the store–aircraft is overdetermined, stiffness elements are also added to yield the ΔK terms of Eq. (14).

Aeroservoelastic Analysis

Various modern ASE, dynamic response and nonlinear analysis techniques require the expression of the aeroelastic equation of motion in a time-domain, state-space, constant coefficient form. For this purpose, the AFC matrices have to be described as rational functions of the arbitrary-motion Laplace variable s. As shown in Ref. 9, the most general rational function approximation of the merged Laplace-domain AFC matrices

$$[Q_h(s)] = [Q_{hh}(s)\, Q_{hc}(s)] \tag{16}$$

that leads to a state-space aeroelastic model can be cast in the form

$$[\tilde{Q}_h(s)] = [A_0] + (b/V)[A_1]s + (b^2/V^2)[A_2]s^2 + [D]([I]s - (V/b)[R])^{-1}[E]s \tag{17}$$

where all the matrix coefficients are real valued. The number of structural states in the resulting state-space model is $2n_h$. The number of aerodynamic states, n_a, is equal to the order of the aerodynamic root matrix $[R]$. Equations (15) and (17) yield the state-space open-loop aeroelastic equation of motion

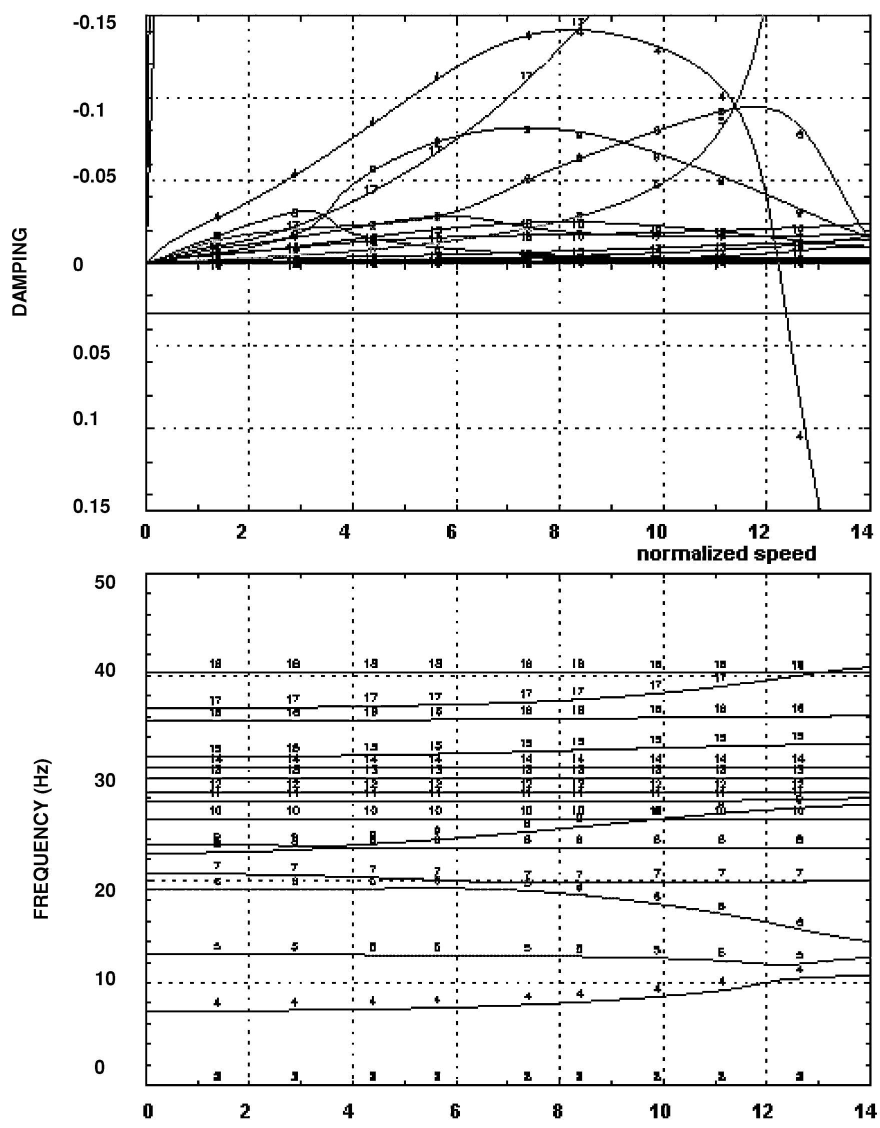

Fig. 9 Frequency and damping variations, clean aircraft by coupling, ASE solution with FCS.

$$\{\dot{x}_{ae}\} = [A_{ae}]\{x_{ae}\} + [B_{ae}]\{u_{ae}\} \tag{18}$$

where

$$\{x_{ae}\} = \begin{Bmatrix} \xi \\ \dot{\xi} \\ x_a \end{Bmatrix} \qquad \{u_{ae}\} = \begin{Bmatrix} \delta_c \\ \dot{\delta}_c \\ \ddot{\delta}_c \end{Bmatrix} \qquad [A_{ae}] = \begin{bmatrix} 0 & I & 0 \\ -[\bar{M}]^{-1}\left[K_{hh} + qA_{hh_0}\right] & -[\bar{M}]^{-1}\left[B_{hh} + \dfrac{qb}{V}A_{hh_1}\right] & -q[\bar{M}]^{-1}[D] \\ 0 & [E_h] & \dfrac{V}{b}[R] \end{bmatrix}$$

$$[B_{ae}] = \begin{bmatrix} 0 & 0 & 0 \\ -q[\bar{M}]^{-1}\left[A_{hc_0}\right] & -\dfrac{qb}{V}[\bar{M}]^{-1}\left[A_{hc_1}\right] & -[\bar{M}]^{-1}\left[M_{hc} + \dfrac{qb^2}{V^2}A_{hc_2}\right] \\ 0 & [E_c] & 0 \end{bmatrix} \qquad [\bar{M}] = [M_{hh}] + \frac{qb^2}{V^2}\left[A_{hh_2}\right]$$

and where $\{x_a\}$ is the vector of aerodynamic augmenting states. Open-loop flutter analysis is performed by simply calculating the eigenvalues of the system matrix $[A_{ae}]$ for various flight conditions and interpolating for the conditions at which one of the eigenvalues crosses to the right side of the Laplace domain.

A control system can be augmented to the states of Eq. (18) as detailed in Ref. 10. The control system can accommodate any combination of single-input/single-output, multi-input/multi-output, and junction elements, interconnected and wired to the sensors and actuators through fixed and variable gains. The gain-open ASE model with the aeroelastic states augmented by those of the actuators and the dynamic control elements is of the form

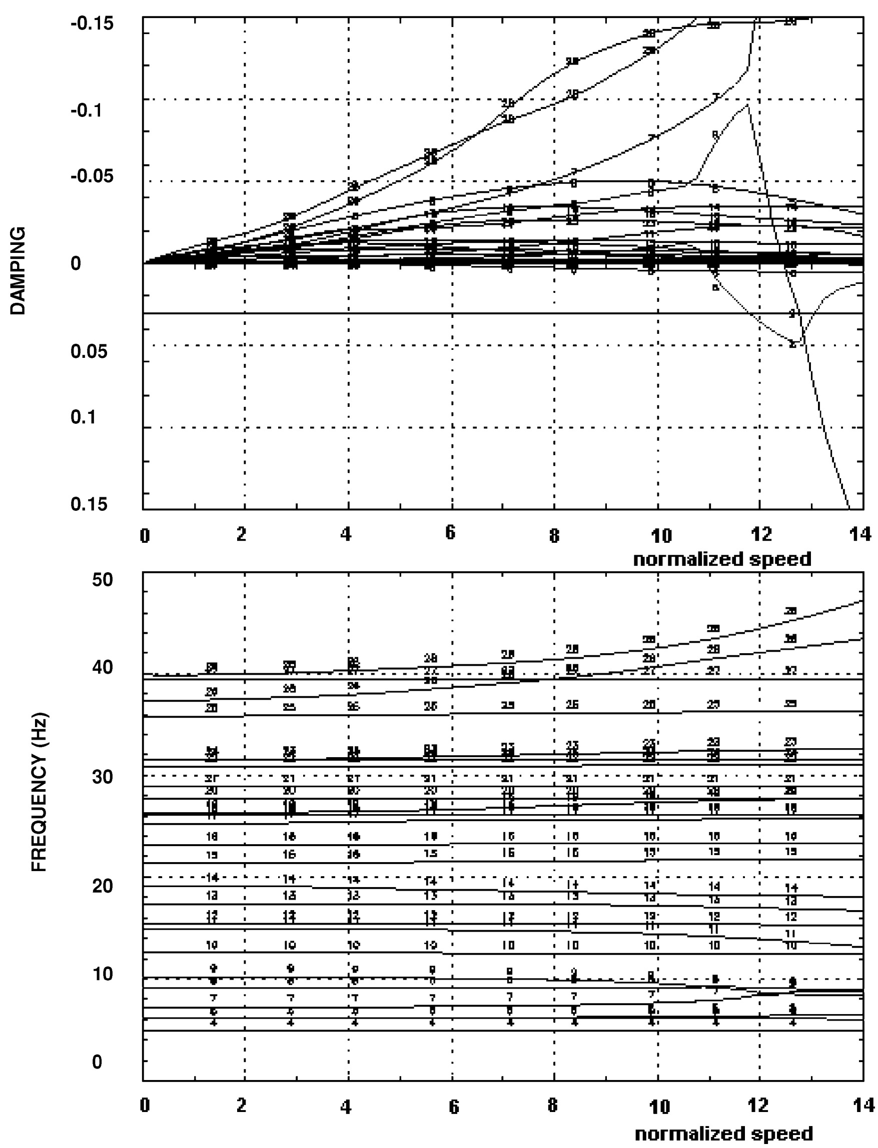

Fig. 10 Frequency and damping vs normalized velocity, aircraft with stores, direct solution.

$$\{\dot{x}_v\} = [A_v]\{x_v\} + [B_v]\{u_v\}, \qquad \{y_v\} = [C_v]\{x_v\} + [D_v]\{u_v\} \quad (19)$$

The ASE loop is closed by relating the input vector $\{u_v\}$ to the output vector $\{y_v\}$ via a gain matrix $[G_v]$,

$$\{u_v\} = [G_v]\{y_v\} \quad (20)$$

which leads to the closed-loop ASE equation of motion

$$\{\dot{x}_v\} = [\bar{A}_v]\{x_v\} \quad (21)$$

The closed-loop flutter characteristics are established by eigenvalue analysis of $[\bar{A}_v]$.

Numerical Examples

The new coupling method is demonstrated for the European Fighter Aircraft model EF-2000 at Mach 0.8 with symmetric boundary conditions. Several superelements representing the main components of the aircraft were extracted from the stress finite element model shown in Fig. 1 and combined for the structural dynamic model. The final model has been matched to ground vibration test (GVT) results. The structural modes were generated with MSC/NASTRAN, and the aeroelastic analyses were performed with ZAERO. Separate flutter analyses were first performed for two reference cases, a clean aircraft (with the tip tanks) and an aircraft with the three store stations loaded with external stores, a full fuel tank, an outboard (O/B) missile, and a stub. The aerodynamic model of the wing with the three stores is shown in Fig. 2.

The stores plus pylons have been modeled by means of stiffness and lumped mass matrices representing their inertial characteristics. The store models have been matched to GVT results. The stores are connected to the aircraft in each of these stations through an overdetermined connection of seven interface coordinates. The model of a typical store and its attachment points is shown in Fig. 3. The forward store-station hard point is attached to the store in all translations and rotations, except yaw. The rear hard point is attached only in the y (side) and z (heave) directions. The store attachment points are connected to those of the wing through attachment springs. The reference store-loaded case was analyzed with the store models added to the aircraft model. It will be shown that accurate flutter results can be produced for the clean aircraft and for various store configurations from a single set of normal modes of the aircraft loaded with fictitious masses instead of actual stores, plus separate clamped store modes. The flutter-by-coupling results will be produced by both the frequency-domain g method and the state-space ASE method.

Normal modes analysis was performed to generate a modal database of the aircraft loaded with fictitious masses at the three store stations. The store models were included in this run, but with the actual store masses removed, the attachment spring connection in pitch at the main hard point removed, and all of the seven interface coordinates loaded with fictitious masses, 10,000 kg in

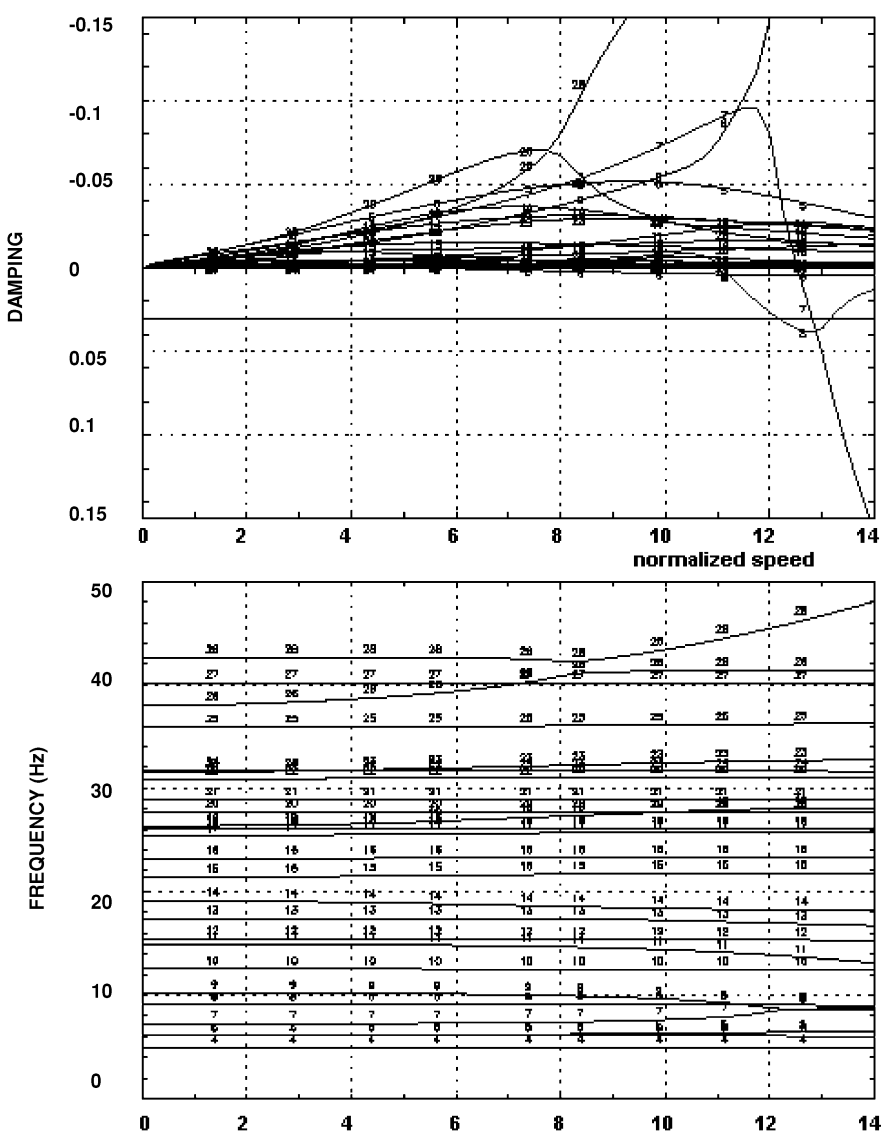

Fig. 11 Frequency and damping vs normalized velocity, aircraft with stores by coupling, ASE solution.

the translation coordinates and 1000 kg · m^2 in the rotation coordinates, at the wing side. A typical store model in this run is shown in Fig. 4. Because the store connections are now statically determined and the stores are without masses, they have no effect on the resulting normal modes. Their presence in the run is convenient because it produces the extrapolated modal displacements $[\phi_{AB}]$ of Eq. (8).

Separate store modes were generated by connecting the relevant store to the ground in a statically determined manner, which leaves the main attachment disconnected in pitch and loaded with a fictitious inertia in this direction, as shown in Fig. 5. The disconnected interface coordinate was selected arbitrarily from the set of three overdetermined connections in plunge and pitch. The resulting modes can be combined with modes of other stores to form $[\phi_B]$ of Eq. (8).

The reference flutter analyses were performed with 34 low-frequency modes taken into account in each case, three of them zero rigid-body frequencies. Previous convergence studies showed that this number of modes is sufficient for obtaining converged flutter results with various store loadings. The database of aircraft modes with fictitious masses at the store stations was constructed with 34 modes, to which 6 clamped modes for each store were added in the aircraft-with-stores case. A comparison between the 15 lowest nonzero natural frequencies, and those obtained by solving the coupling equation (12), are shown in Table 1. Because there are 21 large fictitious masses in the model that generated the aircraft modal database, and because only 34 of these modes are taken into account in the coupling process, it was expected that only the first $34 - 21 = 13$ coupled frequencies of the clean aircraft, namely, 10 elastic frequencies, would be of good accuracy. Indeed, we see in Table 1 that the coupling errors up to the 10th mode in this case are less than 0.55% and start to peak up with higher modes. Some of the coupled frequencies may become very large. These are not natural aircraft modes, but synthetic modes of local deformations near the hard points.

Table 1 Comparison between natural frequencies obtained directly and those obtained by modal coupling

Mode number	Clean aircraft reference	Clean aircraft by coupling	Clean aircraft error, %	Aircraft with stores reference	Aircraft with stores by coupling	Aircraft with stores error, %
1	7.24	7.24	0	4.90	4.92	0.41
2	12.74	12.74	0	6.04	6.04	0
3	19.03	19.06	0.16	6.07	6.07	0
4	20.65	20.71	0.28	7.21	7.22	0.14
5	22.63	22.66	0.13	9.03	9.03	0
6	23.39	23.41	0.09	10.20	10.20	0
7	25.97	25.97	0	12.54	12.54	0
8	27.67	27.68	0.04	14.92	14.92	0
9	28.56	28.61	0.18	15.45	15.46	0.06
10	29.84	30.00	0.54	17.34	17.37	0.17
11	30.78	31.03	0.81	19.10	19.10	0
12	31.48	32.03	1.75	21.35	21.37	0.09
13	34.62	35.54	2.66	23.19	23.20	0.04
14	36.26	36.77	1.41	25.22	25.32	0.40
15	39.49	40.34	2.15	26.04	26.04	0

The coupled flutter results for the clean-aircraft case are compared, in the form of V–g–ω plots, to the direct results in Figs. 6 and 7. Figures 6 and 7, and as shown subsequently, present the variations of structural modal damping g and natural frequencies with the true airspeed, normalized with respect to a reference velocity. The ASE state-space solution method was also used for analyzing open- and closed-loop cases. The open-loop ASE clean-aircraft solution is shown in Fig. 8. The control system effects were analyzed by augmenting the 140-state control system to the aeroelastic plant model. The minimum-state rational aerodynamic method was applied in the ASE cases with 10 aerodynamic roots, with no physical weighting, and with using the default ZAERO approximation options with perfect approximation fit at $k = 0$. The resulting V–g–ω plots are shown in Fig. 9. It can be observed in Figs. 6–9 that, even though there are some differences in the high-damping and high-frequency values, the coupling flutter results are very close to the direct results, definitely within the accuracy level required from such analyses. The high-frequency differences are due to the coupling inaccuracies discussed earlier. Even though the high-frequency aeroelastic behavior obtained by coupling is not accurate, the effects of these modes on the low-frequency flutter mechanisms are still adequate. The open-loop ASE results are practically identical to the frequency-domain G-method results, and control system effects are negligible in this case.

The flutter results of the aircraft with all three external stores, calculated directly by the frequency domain solution and those calculated by modal coupling using the state-space solution, are shown in Figs. 10 and 11, respectively. Here again the coupling results are very close to the direct results. The fact that good coupling results (frequencies and flutter) were obtained for both the clean aircraft and the fully loaded one, based on the same set of fictitious-mass aircraft modes, indicates that other store combinations that involve these store stations can be adequately analyzed as well with this baseline set of modes.

The store aerodynamic effects were analyzed by first applying the model of Fig. 2 to the fully loaded reference case. The variations of modal damping values with normalized velocity are shown in Fig. 12. Note that the severe high-speed flutter case of Fig. 10 is now at a significantly lower velocity (by about 8%). The very

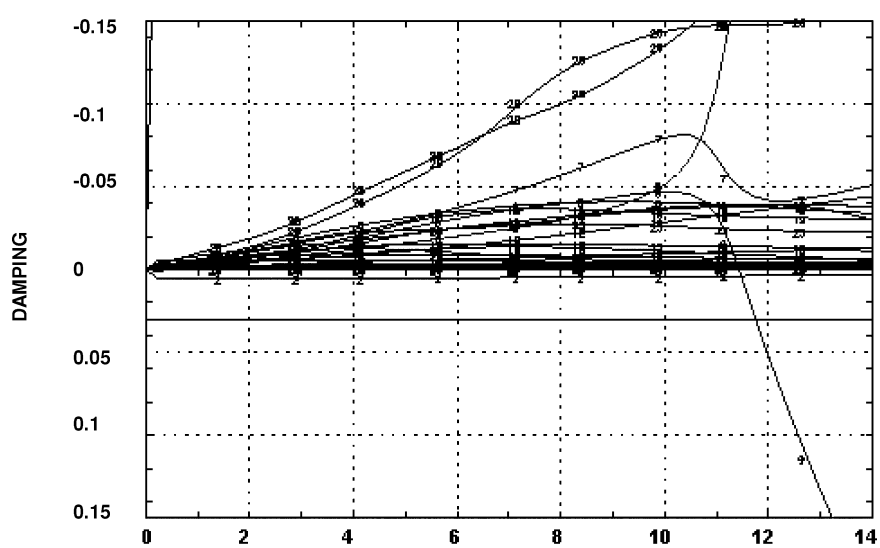

Fig. 12 Damping variations, aircraft with stores, direct solution with store aerodynamics.

Table 2 Summary of normalized flutter speeds and flutter frequencies with store aerodynamic effects

Flutter identification	Wthout Store Aero	Tank Aero	Tank + O/B Aero	Tank + O/B + Stub Aero
		Reference (no coupling)		
S1	4.39 (6.05 Hz)	——	——	——
S2	10.94 (9.20 Hz)	10.68 (9.19 Hz)	——	——
S3	12.45 (8.65 Hz)	12.19 (8.61 Hz)	11.47 (8.88 Hz)	11.43 (8.88 Hz)
		Structural coupling, full aerodynamics		
S1	5.25 (6.05 Hz)	——	——	——
S2	11.09 (9.17 Hz)	10.73 (9.15 Hz)	——	——
S3	12.52 (8.58 Hz)	12.21 (8.55 Hz)	11.46 (8.83 Hz)	11.49 (8.79 Hz)
		Structural and aerodynamics coupling		
S1	N/A	——	——	——
S2	N/A	10.73 (9.15 Hz)	——	——
S3	N/A	12.21 (8.55 Hz)	11.39 (8.86 Hz)	11.36 (8.87 Hz)

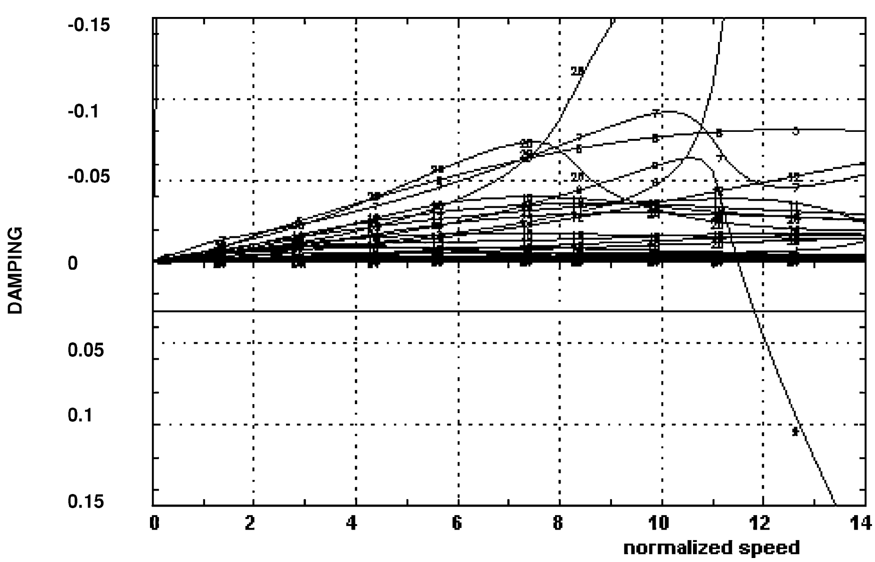

Fig. 13 Damping variations, aircraft with stores, ASE coupling with full store aerodynamics.

mild low-speed flutter mechanism indicated in Fig. 10 by the zero crossing of the damping branch at the normalized velocity of about 6 and the medium-speed hump flutter at the normalized velocity of 11 are stable when store aerodynamics are considered in Fig. 12. The frequency variations are not shown because they are almost identical to those of Fig. 10.

The store aerodynamic effects were also introduced in the ASE coupling analysis, with the aerodynamic panel matrices generated in the reference run of Fig. 12. The resulting damping variations are shown in Fig. 13. They indicate an aeroelastic behavior practically identical to that of Fig. 12. The coupling of separate store aerodynamic effects was performed in two steps. First, the GAF matrices associated with the aircraft and store modes were generated with the aerodynamic shape of each store added to the wing model separately. The subtraction of the clean-aircraft GAF matrices yielded the incremental GAF matrices for each store separately, as shown in Fig. 14. The incremental matrices were then combined in the coupling process.

The damping variations for the three-store case, analyzed by modal coupling of the structural and aerodynamic generalized matrices of each store separately are shown in Fig. 15. The comparison with Fig. 13 indicates negligible effects of the aerodynamic interface between the different stores. A summary of the aerodynamic effects on flutter speeds is shown in Table 2. The effects of the different stores are added one by one, indicating that the missile has the largest aerodynamic effects and the stub has the lowest effect in our numerical example.

Because the number of store cases, with various boundary conditions, Mach numbers, and flight-control-system (FCS) effects, is typically of many thousands, we recommend the following approach when performing repetitive linear flutter analysis.

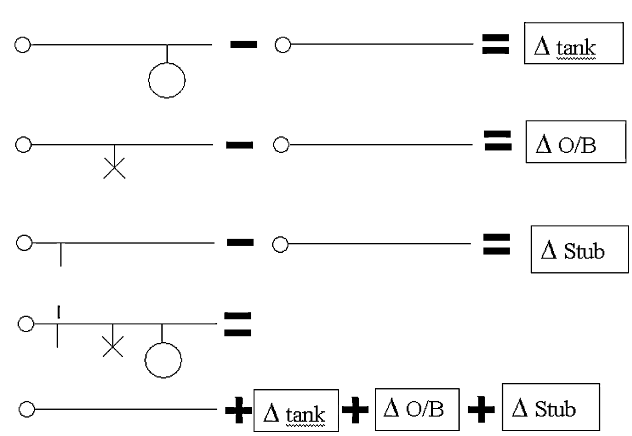

Fig. 14 Defining incremental aerodynamic loads.

1) Construct a database of fictitious-mass clean-aircraft modes and the associated GAF matrices.

2) Construct a database of separate store modes, clamped to the ground.

3) Perform the massive store flutter analyses with the store aerodynamics neglected.

4) Identify the flutter-sensitive store cases.

5) Generate GAF matrices with separate incremental aerodynamic effects of the stores involved in the sensitive cases.

6) Repeat the flutter analyses of the sensitive cases with coupled aerodynamic effects.

7) Identify the most critical cases, typically those selected for ground resonance testing and flutter flight tests, and repeat the

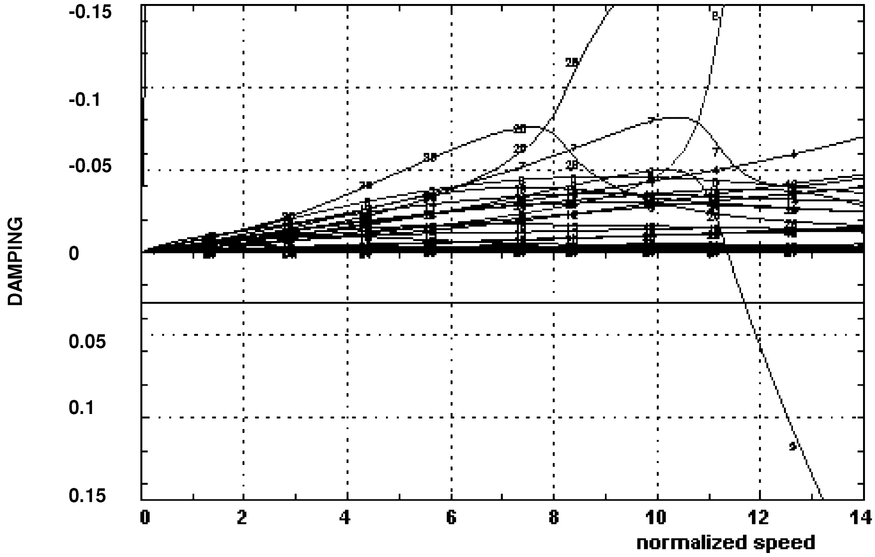

Fig. 15 Damping variations, aircraft with stores, ASE with structural and aerodynamic coupling.

flutter analyses with full aerodynamic interference between stores considered.

Conclusions

The aircraft–store fictitious-mass modal coupling technique was expanded to allow overdetermined store attachments. The method was reformulated to facilitate a convenient application using standard structural perturbation techniques in commercially available codes. The aircraft modal database is determined in a single standard normal-modes analysis with the store attachment coordinates loaded with relatively large fictitious masses. The method is robust to the magnitudes of the fictitious masses, provided those are of the order of the heaviest stores, but not large enough to cause numerical ill conditioning. The method allows varying the actual mass properties of the stores and the stiffness of the attachment springs after the modal database has been constructed. Store aerodynamic effects can be included by either accounting for the full interstore interference, or by coupling the individual effects of each store. The coupled dynamic matrices were used for flutter analysis of two extreme configurations of the EF-2000 aircraft, one without external stores and one loaded with a combination of light and heavy stores at three wing stations, both performed with the same modal database. High-accuracy frequency and flutter results have been demonstrated. The coupling method is applicable with both frequency-domain and state-space methods. The latter allows a convenient inclusion of control systems in ASE and dynamic response analyses. The new technique forms the basis of a numerical process that will perform open- and closed-loop flutter analyses for numerous store-loading cases with a very favorable combination of accuracy and efficiency. The method presented in this paper provides a way to finish efficiently the clearance process of a wide set of different configurations in a timely manner. Furthermore, the generated databases will allow very efficient repetitions of the clearance process in case there is any significant change (from the flutter standpoint) in stiffness and/or mass characteristics in the aircraft standard data and when new external stores are added.

References

[1]Bisplinghoff, R. L., Ashley, H., and Halfman, R. L., *Aeroelasticity*, Addison–Wesley, Reading, MA, 1955, Chap. 9.

[2]Craig, R. R., Jr., and Bampton, M. C. C., "Coupling of Substructures for Dynamic Analysis," *AIAA Journal*, Vol. 6, 1968, pp. 1313–1319.

[3]Karpel, M., and Newman, M., "Accelerated Convergence for Vibration Modes Using the Substructure Coupling Method and Fictitious Coupling Masses," *Israel Journal of Technology*, Vol. 13, May 1975, pp. 55–62.

[4]Karpel, M., "Efficient Vibration Mode Analysis of Aircraft with Multiple External Store Configurations," *Journal of Aircraft*, Vol. 25, No. 8, 1988, pp. 747–751.

[5]Karpel, M., Raveh, D., and Ricci, S., "Ground Vibration Tests of Space-Structure Components Using Boundary Masses," *Journal of Spacecraft and Rockets*, Vol. 33, No. 2, 1996, pp. 272–277.

[6]Karpel, M., and Ricci, S., "Experimental Modal Analysis of Large Structures by Substructuring," *Mechanical Systems and Signal Processing*, Vol. 11, No. 2, 1997, pp. 245–256.

[7]Karpel, M., and Raveh, D., "Fictitious Mass Element in Structural Dynamics," *AIAA Journal*, Vol. 34, No. 3, 1996, pp. 607–613.

[8]ZAERO, Ver. 4.2, Theoretical Manual, ZONA Technology, Scottsdale, AZ, May 2000.

[9]Karpel, M., "Time-Domain Aeroservoelastic Modeling Using Weighted Unsteady Aerodynamic Forces," *Journal of Guidance, Control, and Dynamics*, Vol. 13, No. 1, 1990, pp. 30–37.

[10]Karpel, M., "Reduced-Order Models for Integrated Aeroservoelastic Optimization," *Journal of Aircraft*, Vol. 36, No. 1, 1999, pp. 146–155.